Effects of pressure on the dynamics of an oligomeric protein from deep-sea hyperthermophile

Utsab R. Shrestha[a], Debsindhu Bhowmik[a], John R. D. Copley[b], Madhusudan Tyagi[b,c], Juscelino B. Leão[b], and Xiang-qiang Chu (储祥蔷)[a,1]

[a]Department of Physics and Astronomy, Wayne State University, Detroit, MI 48201; [b]National Institute of Standards and Technology Center for Neutron Research, Gaithersburg, MD 20899; and [c]Department of Materials Science and Engineering, University of Maryland, College Park, MD 20742

Edited by Michael L. Klein, Temple University, Philadelphia, PA, and approved September 28, 2015 (received for review July 23, 2015)

Inorganic pyrophosphatase (IPPase) from *Thermococcus thioreducens* is a large oligomeric protein derived from a hyperthermophilic microorganism that is found near hydrothermal vents deep under the sea, where the pressure is up to 100 MPa (1 kbar). It has attracted great interest in biophysical research because of its high activity under extreme conditions in the seabed. In this study, we use the quasielastic neutron scattering (QENS) technique to investigate the effects of pressure on the conformational flexibility and relaxation dynamics of IPPase over a wide temperature range. The β-relaxation dynamics of proteins was studied in the time ranges from 2 to 25 ps, and from 100 ps to 2 ns, using two spectrometers. Our results indicate that, under a pressure of 100 MPa, close to that of the native environment deep under the sea, IPPase displays much faster relaxation dynamics than a mesophilic model protein, hen egg white lysozyme (HEWL), at all measured temperatures, opposite to what we observed previously under ambient pressure. This contradictory observation provides evidence that the protein energy landscape is distorted by high pressure, which is significantly different for hyperthermophilic (IPPase) and mesophilic (HEWL) proteins. We further derive from our observations a schematic denaturation phase diagram together with energy landscapes for the two very different proteins, which can be used as a general picture to understand the dynamical properties of thermophilic proteins under pressure.

protein dynamics | energy landscape | denaturation phase diagram | quasielastic neutron scattering | mode coupling theory

The biological functions of proteins, such as enzyme catalysis, are often understood from their crystallographic structures (1). On the other hand, it is crucial to take into account dynamic behavior to fully comprehend these functions (2, 3). In vivo, proteins are in constant motion among different conformations (3–5). The thermal energy, which is of the order of k_BT per atom, where k_B is the Boltzmann constant and T is the absolute temperature, triggers biomolecules to sample different conformations around the average structure. These conformations are also known as conformational substates (CSs) (5). Fluctuations among these CSs play an important role in protein function (3, 5). These lead to the concept of a multidimensional potential energy landscape (EL) that specifies a complete description of CSs in proteins (6–9). The existence of an EL was proposed by H. Frauenfelder and others in the 1970s and has been validated both by computations and by experiments (6–12).

Proteins show various dynamic phenomena over a wide range of timescales, from picoseconds to milliseconds (13). A fast dynamic process, on a timescale of a picosecond to 10 ns, also known as β-relaxation, occurs due to small amplitude fluctuations in atoms/molecules, such as loop motions and side-chain rotations (14). The energy barrier or activation energy (E_A) between different CSs for this process is smaller than k_BT (15). On the other hand, slow motions, on the timescale of microseconds to milliseconds mainly occur due to the large-amplitude collective motions such as protein–protein interactions and enzyme catalysis (16). This process, for which the energy barrier separating CSs is much larger than k_BT (14, 15), is called α-relaxation. The fast and slow dynamics of proteins are connected to each other and provide the necessary balance between stability and flexibility required for their enzymatic activity (13). In our study, the quasielastic neutron scattering (QENS) technique was used to investigate the fast dynamics in the picosecond-to-nanosecond time range on the length scale from angstroms to nanometers within the protein secondary structure. Because more than one-half of the atoms in biological macromolecules are hydrogen (H), which has the largest incoherent neutron scattering cross-section (17), incoherent QENS experiments on biological macromolecules predominantly measure the motions of individual H atoms.

Over the past two decades, considerable research effort on protein dynamics has emphasized the effects of temperature and pressure, and has reported significant effects on the motions (18–22). In general, below the physiological temperature limit, the volume of protein molecules increases with increase in temperature due to expansion in the subatomic-sized spaces within the molecules and the hydration layer surrounding the protein (23). Temperature provides conformational flexibility to proteins for enzymatic activities by increasing their conformational fluctuations (24). Nevertheless, sufficiently high temperature may also distort protein structure and cause unfolding or denaturation (25–27). Another thermodynamic parameter, pressure, also plays an important role in protein structure and dynamics (28–33). It changes the protein volume (33) and affects protein intermolecular and intramolecular structures explicitly (28, 32). Evidently, the cavities in folded or native proteins are reduced at high pressure. This perturbs the CSs, giving rise to protein unfolding or denaturation (33–35). Therefore, high temperature and pressure together may prevent enzymatic processes in many biomolecules.

Despite the above, some of the microorganisms found in deep-sea thermal vents are able to resist the effects of high temperature and pressure (36–38). Without any light energy from the sun, these organisms survive, depending on mineral-enriched hydrothermal

Significance

Deep-sea microorganisms can adapt to extreme conditions of high temperature and pressure. What makes these organisms survive and reproduce in such critical conditions remains an open question. Here, we use the quasielastic neutron scattering (QENS) technique to study the dynamic behavior of a hyperthermophilic protein that is found in the deep sea. Our results give evidence that high pressure affects the dynamical properties of proteins by distorting the protein energy landscape in ways that are significantly different for hyperthermophilic and mesophilic proteins. Consequently, a general schematic denaturation phase diagram together with energy landscapes for the two different proteins are derived, and this approach can be used as a general picture to understand the effects of pressure on protein dynamics and activities.

Author contributions: X.-q.C. designed research; U.R.S., D.B., J.R.D.C., M.T., J.B.L., and X.-q.C. performed research; U.R.S. and D.B. analyzed data; and U.R.S., D.B., and X.-q.C. wrote the paper.

The authors declare no conflict of interest.

This article is a PNAS Direct Submission.

[1]To whom correspondence should be addressed. Email: chux@wayne.edu.

This article contains supporting information online at www.pnas.org/lookup/suppl/doi:10.1073/pnas.1514478112/-/DCSupplemental.

fluids, and can perform their metabolic activities, synthesize proteins, and maintain their native conformations. Thus, they engender great interest among researchers in understanding the possible factors or mechanisms that are unique to these living systems, permitting them to survive under such critical circumstances.

One of the deep-sea microorganisms, *Thermococcus thioreducens*, is a hyperthermophilic sulfur-reducing euryarchaeote found in hydrothermal vents of the Mid-Atlantic Ridge under abnormal thermodynamic conditions of high pressure and temperature (39, 40). It lives its life under hydrostatic pressures of about 100 MPa, having an optimal growth temperature range of 356–358 K (83–85 °C) (40). Inorganic pyrophosphatase (IPPase) (enzyme entry EC 3.6.1.1) is an enzyme from this organism, which is of great interest due to its high thermal and biochemical stability (39). It catalyzes the hydrolysis of inorganic pyrophosphate (PP_i) to form orthophosphate (P_i), which helps in several biochemical processes such as nucleic acid polymerization, lipid metabolism, and the production of proteins (39). The static structure of IPPase has recently been overexpressed and characterized by neutron protein crystallography (39). Its quaternary structure is a homohexamer with an oligomeric molecular mass of ∼120 kDa (each subunit is about 20 kDa) (39). Like its mesophile, it has a complicated network of noncovalent interactions that mainly correspond to the interaction of hydrogen bonds (39). However, in contrast to these mesophilic equivalents, this enzyme has the ability to perform catalytic activity at extreme pressures and temperatures. It can resist denaturation even at high temperatures above 348 K (75 °C), and its optimal temperature for enzymatic activity is 358 K (85 °C) (39, 41). From the structure point of view, to form the stabilizing interactions for its quaternary oligomeric structure, IPPase reduces its translational and rotational entropy for the monomers. These interactions include polar/apolar, hydrophobic, ion pairs, and hydrogen bonds between monomers and non–solvent-exposed cavities (41). Therefore, the oligomeric IPPase has a highly symmetric and closed hexameric structure, which makes it stable and biologically active at extreme temperatures and pressures. For comparison, we use a small monomeric protein, hen egg white lysozyme (HEWL) as a model protein. It is a well-studied protein and has been used as a model protein for QENS experiments for decades (14, 42). It consists of 129 amino acid residues that destroy the polysaccharide architecture of bacterial cell walls (43). It catalyzes the hydrolysis of 1,4-β linkages between alternating units of *N*-acetylmuramic acid and *N*-acetylglucosamine. At a pH of 2.0, rapid denaturation in HEWL begins above 320 K (47 °C) and at higher temperatures it loses its enzymatic activity (44). The comparison of enzymatic activities of IPPase and HEWL is shown in Fig. S1 (41, 45). In our previous investigation at ambient pressure with QENS, IPPase was shown to have distinguishably slower dynamics than that of HEWL in the β-relaxation time range of 10 ps to 0.5 ns, which is intimately related to the local flexibility of the oligomeric structure of IPPase (41). Such dynamic behavior was observed at all of the measured temperatures from 220 K (−53 °C) to 353 K (80 °C). It is of great interest to investigate whether the same dynamical behavior holds at high pressure, which reflects the natural living condition of IPPase found in the seabed.

In this study, the relaxation dynamics of both IPPase and HEWL were studied by QENS in two different time ranges on two instruments at the National Institute of Standards and Technology (NIST) Center for Neutron Research (NCNR), in the temperature range from 298 K (25 °C, room temperature) to 363 K (90 °C) at a pressure of 100 MPa, the native environment for IPPase. Due to the limited dynamic range available on the individual instruments, two QENS spectrometers were used to probe the dynamics in a wide time range from subpicoseconds to nanoseconds. Thus, the dynamics in the time range from 2 to 25 ps was measured using the disk chopper time-of-flight spectrometer (DCS) (46) and from 100 ps to 2 ns was determined using the high-flux backscattering spectrometer (HFBS) (47). The experimental results were quantitatively analyzed using two analytical models in both the energy and the time domains. The relaxation dynamics of IPPase and HEWL were directly compared in the time domain. Both proteins demonstrate a nonexponential logarithmic-like decay in their relaxation dynamics. Our results demonstrate that, even though IPPase is a complex oligomeric protein, it continues to preserve its conformation, residual motions, and hence enzymatic activity under high temperature and pressure, which is naturally favorable to these microorganisms. However, our model protein, HEWL, lacks the above in its distinguishable dynamic behavior due to imposed high temperature and pressure. We explain these results based on the highly symmetric and closed oligomeric structure of IPPase, which helps to maintain its native conformation and flexibility under high-pressure and -temperature conditions. We further derive from our experimental observations a scenario of distorted energy landscape of proteins under pressure and a schematic denaturation phase diagram that can be used as a general picture to describe protein dynamics under extreme conditions.

Results and Discussion

Diffusive Motions of Hydrogen Atoms in Protein Molecules, Analyzed in the Energy Domain. Fig. 1 shows the normalized measured self-dynamic incoherent structure factor $S_m(Q, \omega)$, derived from QENS experiments at DCS (*A–D*) and HFBS (*E–H*). Each sample of IPPase and HEWL was hydrated using D_2O to a hydration level $h = 0.37$. Since D_2O has a small neutron incoherent scattering cross-section compared with that of the H atoms within the protein molecules, the QENS signals can be considered to derive from protein contributions only (24, 48). Clearly, the central peaks are broadened from the resolution function, characterizing the quasielastic scattering from the samples. The quasielastic component resembles the diffusive motion or the relaxation process of H atoms within the protein molecules in a confined volume and associated with a protein's conformational flexibility (49, 50). We observe that, for each sample, the higher the temperature, the broader the quasielastic width, implying faster dynamics of the protein molecules. It is clear that the normalized QENS data show faster motions in IPPase than in HEWL at comparable temperatures and length scales. This suggests that IPPase has more conformational flexibility than that of HEWL under 100 MPa of pressure. The QENS data in the energy domain were fitted according to Eq. **S1** in *SI Materials and Methods*. In Fig. 1, the lower four panels show the fitted data along with a linear background at the wave vector transfer $Q = 0.8$ Å^{-1} for the DCS data and at $Q = 0.9$ Å^{-1} for the HFBS data, at $T = 363$ K. The elastic component is represented by a delta function, and the quasielastic component is represented by a Lorentzian function, and both are broadened by the instrumental resolution function. The elastic component in the QENS spectra represents the immobile H atoms; whereas the quasielastic component originates from mobile H atoms in the protein. Half widths at half maximum (HWHMs), designated as $\Gamma(Q)$ of Lorentzians derived from the QENS data for IPPase and HEWL, are calculated from fitting of the measured QENS spectra with Eq. **S1**, and shown in Fig. S2. HWHMs plotted as a function of Q^2 at all of the measured temperatures for IPPase and HEWL, increase with Q^2 and become flat at higher Q values. The Q^2 dependence of the HWHMs suggests diffusive motions of mainly H atoms in a confined volume of space (49, 50). The HWHMs increase with temperature in both protein samples, suggesting an increase in diffusive motion. In addition, the HWHM values are larger for IPPase compared with HEWL, suggesting a faster diffusive process and hence more conformational flexibility in IPPase than in HEWL. The calculated values of the HWHMs are of the order of millielectronvolts (for DCS) to microelectronvolts (for HFBS), representing diffusive processes in the timescale of picoseconds to nanoseconds.

Using the elastic and quasielastic components of the experimental data, an analytical quantity called the elastic incoherent structure factor (EISF) can be derived. It is defined as the fraction of elastic intensity in the QENS spectra (17). Modeling of the EISF provides the geometry of diffusive motions in the protein (49). In Fig. 2 *A–D*, we show the EISFs derived from the QENS measurements as a function of Q at different temperatures for both

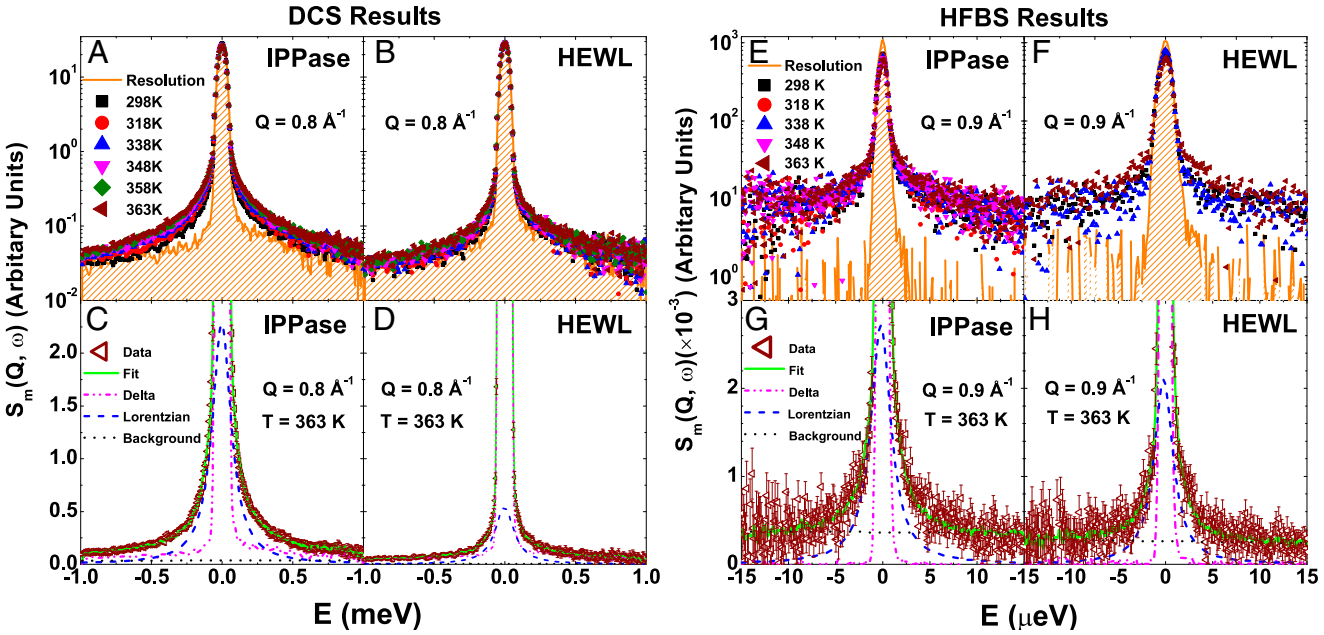

Fig. 1. Normalized QENS spectra from protein samples and data fitting. (*A* and *B*) Spectra measured at DCS from IPPase and HEWL, respectively, at $Q = 0.8$ Å^{-1} for temperatures from 298 to 363 K along with resolution. (*C* and *D*) DCS data fitted in energy domain for IPPase and HEWL, respectively, at $Q = 0.8$ Å^{-1} and $T = 363$ K. (*E* and *F*) Spectra measured at HFBS from IPPase and HEWL, respectively, at $Q = 0.9$ Å^{-1} for temperatures from 298 to 363 K along with resolution. (*G* and *H*) HFBS data fitted in energy domain for IPPase and HEWL, respectively, at $Q = 0.9$ Å^{-1} and $T = 363$ K. The background is fitted linearly, and elastic and quasielastic components are fitted with delta and Lorentzian functions, respectively. In this figure, and in subsequent figures, error bars represent ±1 SD.

IPPase and HEWL. The details of the EISF calculation from energy domain data and its verification with the EISF as calculated from time domain data (as shown in Fig. S3) are provided in *SI Materials and Methods*. The decrease in the EISF with increase in temperature for both proteins suggests that the fraction of immobile H atoms decreases with increase in temperature. EISF curves are fitted well with the expression for single diffusive motion of atoms within a sphere. According to this model, each atom diffuses freely within an impermeable sphere (17, 49, 51). The complete expression for the model can be written as follows: EISF $= p_0 + (1 - p_0)(3j_1(Qa)/Qa)^2$, where $j_1(Qa)$, p_0, and a denote the spherical Bessel function of the first kind of order 1, the elastic fraction, and the radius of the diffusion sphere, respectively.

The fractions of mobile H atoms, $1 - p_0$ for the two proteins are plotted in Fig. 2 *E* and *F*, as functions of temperature, calculated from DCS and HFBS data, respectively. It is clear that the population of mobile H atoms, $1 - p_0$, is much higher for IPPase than for HEWL at all temperatures, indicating that more mobile H atoms in IPPase are observable within our measurement's dynamic window. This result is consistent for the data obtained at both instruments. Moreover, the increase in $1 - p_0$ with increase of temperature indicates that more H atoms are in motion as the temperature rises. Also, the fitting parameter a is listed in Table S1 and explained briefly in *SI Materials and Methods*.

Relaxation Dynamics of Proteins Analyzed in the Time Domain. The intermediate scattering function (ISF) $I(Q, t)$ in the time domain is calculated by taking the inverse Fourier transform of the measured self-dynamic incoherent structure factor $S_m(Q, \omega)$ divided by the inverse Fourier transform of the resolution function $R(Q, \omega)$, as described in detail in *SI Materials and Methods*. The ISF is also known as the single-particle correlation function, and is normally used as an essential tool to describe the relaxation dynamics in protein molecules. It is also the primary quantity of theoretical interest related to the experiment (14, 15, 17, 52). Previous studies show that proteins share similar dynamic features as glass forming liquids (53–56) that can be described by mode coupling theory (MCT) (15, 57). The MCT has successfully predicted a nonexponential logarithmic-like decay in the β-relaxation region (picoseconds to nanoseconds) of protein dynamics, and has proved effective in explaining protein dynamical behavior both in experiments and in molecular dynamics (MD) simulations (14, 15, 24, 41, 58). Therefore, the nonexponential relaxation dynamics in the ISF can be analyzed using an asymptotic expression derived from the MCT (see details in *SI Materials and Methods*) (15):

$$I(Q,t) \sim f(Q,T) - H_1(Q,T)\ln\left(t/\tau_\beta(T)\right) + H_2(Q,T)\ln^2\left(t/\tau_\beta(T)\right), \quad [1]$$

where $f(Q, T)$ is a Q-dependent prefactor, proportional to the Debye–Waller factor for small Q, and $\tau_\beta(T)$ is the characteristic β-relaxation time, which is a Q-independent parameter. $H_1(Q, T)$

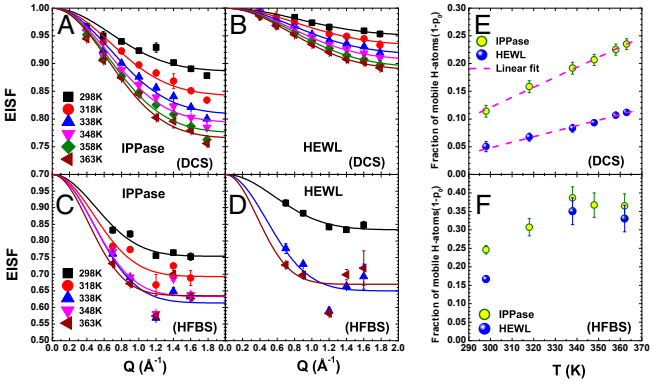

Fig. 2. Analysis of QENS data in the energy domain at all measured temperatures. (*A* and *B*) Elastic incoherent structure factor (EISF) for IPPase and HEWL, calculated from the data measured at DCS. (*C* and *D*) EISFs calculated from the data obtained at HFBS. (*E* and *F*) Fraction of mobile H atoms in a confined diffusion sphere ($1 - p_0$) as a function of temperature for IPPase (yellow circles) and HEWL (blue spheres), calculated from the data obtained at DCS and HFBS, respectively.

and $H_2(Q, T)$ are first- and second-order logarithmic decay parameters, respectively, from the model.

In Fig. 3, the ISFs for IPPase and HEWL are plotted and analyzed at three temperatures T = 298, 338, and 363 K at Q values from 0.5 to 1.8 Å^{-1}. The left and right panels demonstrate the ISFs calculated from QENS data measured at DCS and HFBS, respectively, in the β-relaxation region. One observes an apparent logarithmic-like relaxation process for both proteins in the measured time range. This nonexponential dynamic behavior has been observed in proteins and other biopolymers in many previous studies (14, 15, 24, 41, 58). The ISFs are fitted according to Eq. **1**, and fitted curves are shown in Fig. 3 with solid lines. We obtain four fitting parameters, $A(T)$, $\tau_\beta(T)$, $H_1(Q, T)$, and $H_2(Q, T)$ by global fitting at all six Q values, where $A(T)$ comes from the Debye–Waller factor (see *SI Materials and Methods* for details). In Fig. 4 *A* and *B*, $H_1(Q, T)$ as a function of Q at all temperatures for IPPase and HEWL are respectively plotted. $H_1(Q, T)$ represents qualitatively the slope of the decay, or the power of decay, and can be further fitted by a power law of Q given by Eq. **S7**, $H_1(Q, T) = B_1(T)Q^b$, where b has a value between 1 and 2 for small Qs, and $B_1(T)$ is a temperature-dependent parameter, shown in the *Inset* of Fig. 4*B* for both proteins. Evidently $B_1(T)$ is larger for IPPase than for HEWL at all temperatures and increases linearly with increase in temperature, implying larger flexibility in IPPase than in HEWL in the measured energy/time window. The characteristic β-relaxation time $\tau_\beta(T)$ is plotted vs. 1,000/T (the so-called Arrhenius plot) in Fig. 4*C*. The relaxation times can be fitted using the Arrhenius expression, $\tau_\beta(T) = \tau_0 \exp(E_A/k_BT)$, where E_A is the activation energy that enables conformational transition across energy barriers between CSs. This result is consistent with our previous observations of the relaxation time in other proteins including IPPase and HEWL, at temperatures higher than 300 K and at ambient pressure (24, 41, 58). The calculated values of activation energy E_A from the Arrhenius law are 30 ± 4 meV and 43 ± 4 meV for IPPase and HEWL, respectively, slightly higher than the thermal energy k_BT at room temperature, which is ∼25 meV. These values correspond to the low-frequency modes of excitations in proteins that are perceptible in the β-relaxation process (14, 59). The larger value of E_A for HEWL suggests more rigidity due to unfolding/denaturation compared with IPPase at 100-MPa pressure. The astonishing observation is that the β-relaxation time $\tau_\beta(T)$ is smaller for IPPase than for HEWL at all of the measured temperatures, contrary to what we observed at ambient pressure (41).

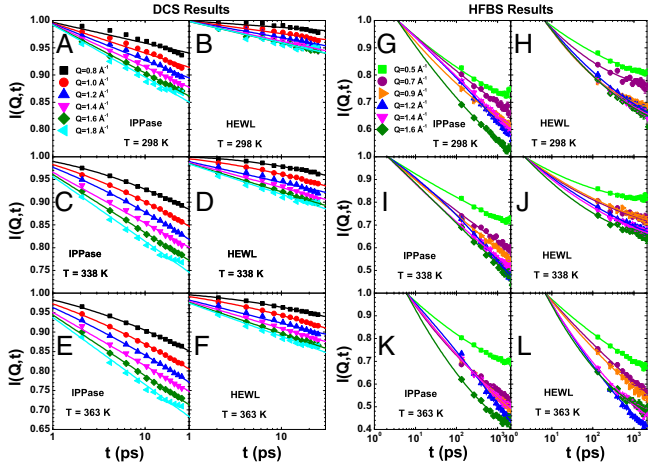

Fig. 3. Intermediate scattering function (ISF) calculated from DCS and HFBS spectra. (*A*–*F*) ISFs of H atoms in hydrated IPPase (*A*, *C*, and *E*) and HEWL (*B*, *D*, and *F*), respectively, calculated from DCS data. (*G*–*L*) ISFs of H atoms in hydrated IPPase (*G*, *I*, and *K*) and HEWL (*H*, *J*, and *L*), respectively, calculated from HFBS data. Here, we show results at three temperatures: T = 298, 338, and 363 K. ISFs are calculated at a series of Q values from 0.5 to 1.8 Å^{-1}. Solid lines represent the curves fitted by Eq. **1**.

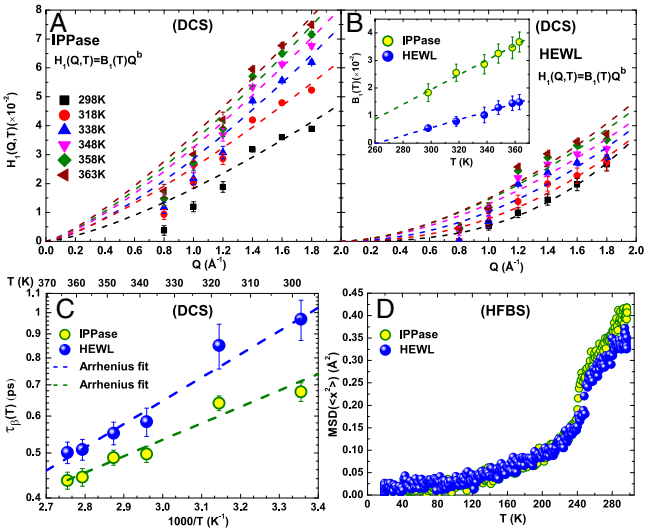

Fig. 4. Fitting parameters obtained from the MCT analysis of the ISF from DCS data and mean-squared displacement (MSD) of IPPase and HEWL from HFBS data. (*A* and *B*) First-order logarithmic decay parameter $H_1(Q, T)$ as a function of Q for IPPase and HEWL, respectively. (*Inset*) $B_1(T)$ as a function of temperature for IPPase and HEWL. (*C*) β-Relaxation time constant, $\tau_\beta(T)$ plotted as a function of temperature. Dashed lines represent Arrhenius fit of the relaxation time τ_β for IPPase and HEWL. (*D*) MSD (<x^2>) of H atoms in protein samples, IPPase and HEWL, measured by elastic incoherent neutron scattering at HFBS. The dynamic transition temperature (T_D) for IPPase and HEWL are observed around 220–240 K.

The Mean-Squared Displacement and Protein Flexibility Under Pressure. Fig. 4*D* shows the mean-squared displacement (MSD), <x^2>, of H atoms in the protein samples, calculated from the elastic incoherent neutron scattering data measured at HFBS. The calculation of MSD is discussed in *SI Materials and Methods*. From the MSD vs. temperature plot, changes in the slopes of both curves indicate that both proteins undergo a dynamic transition at a temperature T_D around 220–240 K, as observed in many other experiments (24, 41, 60–62). The dynamic transition temperature T_D can be considered as the lowest temperature that enables proteins to have the necessary flexibility for different CSs. Our observed T_D value at high pressure is consistent with previous observations at ambient pressure (41). Therefore, the dynamic transition appears to be pressure independent, which is consistent with previous MD simulation results (63). However, a significant difference between the MSDs of IPPase and HEWL is observed above T_D at 100 MPa, which is completely different from the nearly identical MSDs of IPPase and HEWL observed at ambient pressure (41). This contrast in MSDs is due to a pressure induced effect on the CSs of the proteins, which causes a change in the flexibility of the two proteins above T_D. This observation is consistent with a recently published MD simulation calculation (64). Here, we observe a smaller slope of the MSD in HEWL above T_D, which is proportional to the structural resilience of the protein (65, 66), implying that HEWL has increased stability (greater rigidity) and decreased activity, i.e., it loses its conformational flexibility due to pressure-induced unfolding. At the same time, IPPase tends to maintain its conformational flexibility under the same high pressure.

The Pressure Effect on Protein Dynamics and the Scenario of Distorted Energy Landscapes. Our results indicate that pressure affects the dynamics of proteins and therefore brings about a reversal in the dynamical behavior of two protein samples at high pressure from ambient pressure (41). Previous MD simulations have addressed the effect of pressure on protein ELs and have suggested that an invariant description of protein ELs should be subsumed by a fluctuating picture (63). Fig. 5 shows schematic pictures of the denaturation phase diagram and ELs for both proteins, based upon our experimental results with respect to pressure and temperature (21, 30). In Fig. 5, *Left*, IPPase has a larger region of folded state in

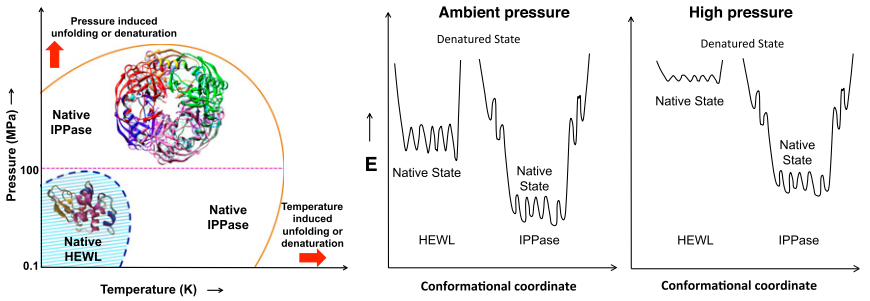

Fig. 5. Schematic picture of phase diagram and energy landscape in IPPase and HEWL under high pressure and temperature. (*Left*) Denaturation phase diagram of IPPase and HEWL (shaded region) as functions of temperature and pressure. The axes in the diagram are not drawn to scale. (*Right*) Schematic plot of cross-sections through a highly simplified energy landscape of atomic fluctuations for different conformational substates (CSs) in IPPase and HEWL under ambient and 100 MPa (1 kbar) of pressure.

the phase diagram compared with HEWL (shaded region with cyan lines). The magenta dashed line shows the outline of our current measurements at 100 MPa. This phase diagram clearly demonstrates that, along the magenta dashed line, HEWL is unfolded/denatured at 100 MPa at all of the measured temperatures, whereas IPPase remains in its native state until a relatively high temperature of 363 K (90 °C). On the other hand, in our previous measurements at ambient pressure (41), both proteins were at their native states below 320 K. This explains why the dynamical behaviors of the two proteins are completely reversed at high pressures of 100 MPa compared with ambient pressure.

The right two panels of Fig. 5 represent the schematic ELs of atomic fluctuations in IPPase and HEWL at ambient pressure and at a pressure of 100 MPa. Previous studies reported that pressure causes a decrease in the length of hydrogen bonds that are formed by backbone amide groups to carbonyl groups or surrounding water molecules, which shrinks the cavities in the native/folded state (67). Such a reduction in the volume of cavities (33, 67, 68), induced by pressure, will further cause changes in protein conformations (69). Therefore, a change in volume of the cavities will agitate different CSs within the protein ensemble and hence distort the ELs. At high pressure, the ELs of a mesophilic protein such as HEWL are largely affected, resulting in a decrease of energy barriers between the native and denatured states. This makes it easy to cross the energy barrier to reach the unfolded/denatured state irreversibly, even at room temperature. On the other hand, the ELs of IPPase are also distorted by high pressure of 100 MPa, but the energy barriers between the native and denatured states are still high enough to sustain its conformational flexibility in its native state.

In general, high pressure dissociates the subunits of oligomers and destabilizes the protein, but the interesting aspect here is to understand why IPPase, an oligomeric protein, reflects physiological dynamic behavior under high pressure. This can be explained by assuming that cavities inside the protein are not disturbed due to its highly symmetric and closed oligomeric structure, which helps to maintain its native conformation and flexibility under high pressure as well as temperature. Previous work has also studied the enzymatic functions of several hyperthermophiles from the deep sea and found that they demonstrate higher rates of enzymatic activity at high pressure and temperature than that of simple monomeric proteins under the same conditions (38). This exotic property of specific proteins such as IPPase enables some microorganisms to defy the effects of high pressure and temperature to sustain their lives under the deep seabed (70).

Conclusion

In summary, our study reveals the effects of pressure on a large hyperthermophilic oligomeric protein IPPase and shows how it steadily maintains its conformational and dynamic properties in its native environment at high temperature and pressure. Also, our results indicate that, under a pressure of 100 MPa, IPPase displays much faster relaxation dynamics than a mesophilic model protein, HEWL, at all of the measured temperatures, opposite to what we have observed previously under ambient pressure (41).

In addition, our experimental results indicate that pressure drives the volume reduction of intramolecular spacing (69) that causes mesophilic HEWL to lose its conformational flexibility as suggested by MSD results, and consequently, its catalytic activity. However, the hyperthermophilic protein IPPase is able to preserve its conformational flexibility and maintain its enzymatic activity at high pressure and temperature, supposedly due to its highly symmetric and closed oligomeric structure. Furthermore, we investigated the relaxation dynamics of proteins in the β-relaxation region in the time domain, vital to their biological activities. Both proteins follow a nonexponential logarithmic-like decay in the ISF as suggested by MCT for glass-forming liquids. The relaxation dynamics due to diffusion of H atoms in the time range of picoseconds to nanoseconds, decays more rapidly in IPPase than in HEWL at respective temperature under high pressure, opposite to what we observed under ambient pressure (41). This dynamic reversal can be explained by a general schematic denaturation phase diagram together with ELs for the two proteins. Such a scenario can be further used as a general picture to understand the functional activities of thermophilic proteins under pressure. Our observation also strongly supports the hypothesis that the protein ELs are distorted by high pressure (28, 63), which are significantly different for hyperthermophilic (IPPase) and mesophilic (HEWL) proteins.

Materials and Methods

Sample Preparation. Both IPPase and HEWL samples were purchased from iXpressGenes. The expression and purification processes of IPPase are briefly described in *SI Materials and Methods*. The HEWL sample was used without further purification. Before exposing to neutrons, the lyophilized IPPase and HEWL powder samples were hydrated with D_2O with hydration level $h = 0.37$. Overnight hydration was performed by placing the powder samples with D_2O vapor inside a glove box. The hydration level enables the protein to maintain its activity with at least a monolayer of D_2O covering its surface (71).

QENS. QENS experiments were performed using DCS (46) and HFBS (47) at NCNR. The DCS was operated at 6 Å, at which wavelength its energy resolution was 64 μeV (full width at half maximum), and a dynamic range suitable for our QENS data analysis of ±1.0 meV. The other spectrometer HFBS has an energy resolution of 0.8 μeV (FWHM, for the Q-averaged resolution value) and a dynamic range of ±17 μeV. The QENS measurements were performed at 100 MPa (1 kbar), at six temperatures ranging from 298 K (25 °C, room temperature) to 363 K (90 °C), in a wave vector transfer range from $Q = 0.4$ to 1.8 $Å^{-1}$. The resolution function at HFBS was measured at 4 K, and that at DCS was from the measurement of a vanadium standard sample, where most of the signal is completely elastic. The elastic scattering data were obtained by performing fixed window scans at HFBS from 298 K down to 19 K, with a ramp rate of 1 K/min. In this mode, the Doppler drive (and therefore the monochromator) is stopped and only neutrons with the same final and initial energies are counted. High pressure was achieved using a commercially available two-stage helium intensifier. The samples were loaded into an aluminum alloy vessel with an inner sample space of 1.5 cm^3. The pressure vessel was connected to the intensifier through a high-pressure capillary. Pressure was adjusted only at temperatures well above the melting curve of helium. Details of the QENS data analysis are available in *SI Materials and Methods*.

ACKNOWLEDGMENTS. We appreciate technical support from Drs. Yiming Qiu and Wei Zhou during the neutron scattering experiments at the National Institute of Standards and Technology (NIST) Center for Neutron Research. We are also grateful to Dr. Joseph D. Ng and Manavalan Gajapathy at the University of Alabama in Huntsville, and to Drs. Hugh M. O'Neill and Qiu Zhang at Oak Ridge National Laboratory for their help with sample preparation. This project was funded and supported by Wayne State University. This work used facilities supported in part by the National Science Foundation under Agreement DMR-1508249.

1. Orengo CA, Todd AE, Thornton JM (1999) From protein structure to function. *Curr Opin Struct Biol* 9(3):374–382.
2. Frauenfelder H, et al. (2009) A unified model of protein dynamics. *Proc Natl Acad Sci USA* 106(13):5129–5134.
3. Henzler-Wildman K, Kern D (2007) Dynamic personalities of proteins. *Nature* 450(7172): 964–972.
4. Parak F, Knapp EW (1984) A consistent picture of protein dynamics. *Proc Natl Acad Sci USA* 81(22):7088–7092.
5. Frauenfelder H, Parak F, Young RD (1988) Conformational substates in proteins. *Annu Rev Biophys Biophys Chem* 17:451–479.
6. Frauenfelder H, Leeson DT (1998) The energy landscape in non-biological and biological molecules. *Nat Struct Biol* 5(9):757–759.
7. Frauenfelder H, Sligar SG, Wolynes PG (1991) The energy landscapes and motions of proteins. *Science* 254(5038):1598–1603.
8. Austin RH, Beeson KW, Eisenstein L, Frauenfelder H, Gunsalus IC (1975) Dynamics of ligand binding to myoglobin. *Biochemistry* 14(24):5355–5373.
9. Onuchic JN, Luthey-Schulten Z, Wolynes PG (1997) Theory of protein folding: The energy landscape perspective. *Annu Rev Phys Chem* 48:545–600.
10. Hofmann C, Aartsma TJ, Michel H, Köhler J (2003) Direct observation of tiers in the energy landscape of a chromoprotein: A single-molecule study. *Proc Natl Acad Sci USA* 100(26):15534–15538.
11. Kitao A, Hayward S, Go N (1998) Energy landscape of a native protein: Jumping-among-minima model. *Proteins* 33(4):496–517.
12. Milanesi L, et al. (2012) Measurement of energy landscape roughness of folded and unfolded proteins. *Proc Natl Acad Sci USA* 109(48):19563–19568.
13. Henzler-Wildman KA, et al. (2007) A hierarchy of timescales in protein dynamics is linked to enzyme catalysis. *Nature* 450(7171):913–916.
14. Chu XQ, et al. (2010) Experimental evidence of logarithmic relaxation in single-particle dynamics of hydrated protein molecules. *Soft Matter* 6(12):2623–2627.
15. Lagi M, Baglioni P, Chen SH (2009) Logarithmic decay in single-particle relaxation of hydrated lysozyme powder. *Phys Rev Lett* 103(10):108102.
16. Mulder FAA, Hon B, Mittermaier A, Dahlquist FW, Kay LE (2002) Slow internal dynamics in proteins: Application of NMR relaxation dispersion spectroscopy to methyl groups in a cavity mutant of T4 lysozyme. *J Am Chem Soc* 124(7):1443–1451.
17. Gabel F, et al. (2002) Protein dynamics studied by neutron scattering. *Q Rev Biophys* 35(4):327–367.
18. Calandrini V, Kneller GR (2008) Influence of pressure on the slow and fast fractional relaxation dynamics in lysozyme: A simulation study. *J Chem Phys* 128(6):065102.
19. Chu XQ, et al. (2009) Proteins remain soft at lower temperatures under pressure. *J Phys Chem B* 113(15):5001–5006.
20. Filabozzi A, et al. (2010) Elastic incoherent neutron scattering as a probe of high pressure induced changes in protein flexibility. *Biochim Biophys Acta* 1804(1):63–67.
21. Heremans K, Smeller L (1998) Protein structure and dynamics at high pressure. *Biochim Biophys Acta* 1386(2):353–370.
22. Mamontov E, O'Neill H, Zhang Q, Chathoth SM (2013) Temperature dependence of the internal dynamics of a protein in an aqueous solvent: Decoupling from the solvent viscosity. *Chem Phys* 424:12–19.
23. Tilton RF, Jr, Dewan JC, Petsko GA (1992) Effects of temperature on protein structure and dynamics: X-ray crystallographic studies of the protein ribonuclease-A at nine different temperatures from 98 to 320 K. *Biochemistry* 31(9):2469–2481.
24. Dhindsa GK, Tyagi M, Chu XQ (2014) Temperature-dependent dynamics of dry and hydrated β-casein studied by quasielastic neutron scattering. *J Phys Chem B* 118(37):10821–10829.
25. Day R, Bennion BJ, Ham S, Daggett V (2002) Increasing temperature accelerates protein unfolding without changing the pathway of unfolding. *J Mol Biol* 322(1):189–203.
26. Khechinashvili NN, Janin J, Rodier F (1995) Thermodynamics of the temperature-induced unfolding of globular proteins. *Protein Sci* 4(7):1315–1324.
27. Meersman F, et al. (2010) Consistent picture of the reversible thermal unfolding of hen egg-white lysozyme from experiment and molecular dynamics. *Biophys J* 99(7):2255–2263.
28. Frauenfelder H, et al. (1990) Proteins and pressure. *J Phys Chem* 94(3):1024–1037.
29. Mozhaev VV, Heremans K, Frank J, Masson P, Balny C (1996) High pressure effects on protein structure and function. *Proteins* 24(1):81–91.
30. Gross M, Jaenicke R (1994) Proteins under pressure: The influence of high hydrostatic pressure on structure, function and assembly of proteins and protein complexes. *Eur Biophys J* 221(2):617–630.
31. Li H, Yamada H, Akasaka K (1999) Effect of pressure on the tertiary structure and dynamics of folded basic pancreatic trypsin inhibitor. *Biophys J* 77(5):2801–2812.
32. Boonyaratanakornkit BB, Park CB, Clark DS (2002) Pressure effects on intra- and intermolecular interactions within proteins. *Biochim Biophys Acta* 1595(1-2):235–249.
33. Roche J, et al. (2012) Cavities determine the pressure unfolding of proteins. *Proc Natl Acad Sci USA* 109(18):6945–6950.
34. Prehoda KE, Mooberry ES, Markley JL (1998) Pressure denaturation of proteins: Evaluation of compressibility effects. *Biochemistry* 37(17):5785–5790.
35. Hillson N, Onuchic JN, García AE (1999) Pressure-induced protein-folding/unfolding kinetics. *Proc Natl Acad Sci USA* 96(26):14848–14853.
36. Daniel I, Oger P, Winter R (2006) Origins of life and biochemistry under high-pressure conditions. *Chem Soc Rev* 35(10):858–875.
37. Stetter KO (2006) Hyperthermophiles in the history of life. *Philos Trans R Soc Lond B Biol Sci* 361(1474):1837–1842, discussion 1842–1843.
38. Ohmae E, Murakami C, Gekko K, Kato C (2007) Pressure effects on enzyme functions. *J Biol Macromol* 7:23–29.
39. Hughes RC, et al. (2012) Inorganic pyrophosphatase crystals from *Thermococcus thioreducens* for X-ray and neutron diffraction. *Acta Crystallogr Sect F Struct Biol Cryst Commun* 68(Pt 12):1482–1487.
40. Byrne-Steele ML, Ng JD (2009) Expression, purification and preliminary X-ray analysis of proliferating cell nuclear antigen from the archaeon *Thermococcus thioreducens*. *Acta Crystallogr Sect F Struct Biol Cryst Commun* 65(Pt 9):906–909.
41. Chu XQ, et al. (2012) Dynamic behavior of oligomeric inorganic pyrophosphatase explored by quasielastic neutron scattering. *J Phys Chem B* 116(33):9917–9921.
42. Roh JH, et al. (2006) Influence of hydration on the dynamics of lysozyme. *Biophys J* 91(7):2573–2588.
43. Carrillo W, García-Ruiz A, Recio I, Moreno-Arribas MV (2014) Antibacterial activity of hen egg white lysozyme modified by heat and enzymatic treatments against oenological lactic acid bacteria and acetic acid bacteria. *J Food Prot* 77(10):1732–1739.
44. Matthyssens GE, Simons G, Kanarek L (1972) Study of the thermal-denaturation mechanism of hen egg-white lysozyme through proteolytic degradation. *Eur J Biochem* 26(4):449–454.
45. Hikima S, Hikima J-i, Rojtinnakorn J, Hirono I, Aoki T (2003) Characterization and function of kuruma shrimp lysozyme possessing lytic activity against *Vibrio* species. *Gene* 316:187–195.
46. Copley JRD, Cook JC (2003) The Disk Chopper Spectrometer at NIST: A new instrument for quasielastic neutron scattering studies. *Chem Phys* 292(2-3):477–485.
47. Meyer A, Dimeo RM, Gehring PM, Neumann DA (2003) The high-flux backscattering spectrometer at the NIST Center for Neutron Research. *Rev Sci Instrum* 74(5):2759–2777.
48. Nickels JD, et al. (2012) Dynamics of protein and its hydration water: Neutron scattering studies on fully deuterated GFP. *Biophys J* 103(7):1566–1575.
49. Fujiwara S, Plazanet M, Matsumoto F, Oda T (2011) Internal motions of actin characterized by quasielastic neutron scattering. *Eur Biophys J* 40(5):661–671.
50. Dellerue S, Petrescu A-J, Smith JC, Bellissent-Funel M-C (2001) Radially softening diffusive motions in a globular protein. *Biophys J* 81(3):1666–1676.
51. Volino F, Dianoux AJ (1980) Neutron incoherent scattering law for diffusion in a potential of spherical symmetry: General formalism and application to diffusion inside a sphere. *Mol Phys* 41(2):271–279.
52. Kneller GR (2005) Quasielastic neutron scattering and relaxation processes in proteins: Analytical and simulation-based models. *Phys Chem Chem Phys* 7(13):2641–2655.
53. Angell CA (1995) Formation of glasses from liquids and biopolymers. *Science* 267(5206): 1924–1935.
54. Etchegoin P (1998) Glassylike low-frequency dynamics of globular proteins. *Phys Rev E Stat Phys Plasmas Fluids Relat Interdiscip Topics* 58(1):845–848.
55. Iben IE, et al. (1989) Glassy behavior of a protein. *Phys Rev Lett* 62(16):1916–1919.
56. Green JL, Fan J, Angell CA (1994) The protein-glass analogy: Some insights from homopeptide comparisons. *J Phys Chem* 98(51):13780–13790.
57. Gotze W, Sjogren L (1992) Relaxation processes in supercooled liquids. *Rep Prog Phys* 55(3):241–376.
58. Chu XQ, Mamontov E, O'Neill H, Zhang Q (2013) Temperature dependence of logarithmic-like relaxational dynamics of hydrated tRNA. *J Phys Chem Lett* 4(6):936–942.
59. Chou K-C (1985) Low-frequency motions in protein molecules. β-Sheet and β-barrel. *Biophys J* 48(2):289–297.
60. Rasmussen BF, Stock AM, Ringe D, Petsko GA (1992) Crystalline ribonuclease A loses function below the dynamical transition at 220 K. *Nature* 357(6377):423–424.
61. Ringe D, Petsko GA (2003) The "glass transition" in protein dynamics: What it is, why it occurs, and how to exploit it. *Biophys Chem* 105(2-3):667–680.
62. Caliskan G, et al. (2006) Dynamic transition in tRNA is solvent induced. *J Am Chem Soc* 128(1):32–33.
63. Meinhold L, Smith JC, Kitao A, Zewail AH (2007) Picosecond fluctuating protein energy landscape mapped by pressure temperature molecular dynamics simulation. *Proc Natl Acad Sci USA* 104(44):17261–17265.
64. Calligari PA, et al. (2015) Adaptation of extremophilic proteins with temperature and pressure: Evidence from initiation factor 6. *J Phys Chem B* 119(25):7860–7873.
65. Zaccai G (2000) How soft is a protein? A protein dynamics force constant measured by neutron scattering. *Science* 288(5471):1604–1607.
66. Tehei M, Daniel R, Zaccai G (2006) Fundamental and biotechnological applications of neutron scattering measurements for macromolecular dynamics. *Eur Biophys J* 35(7):551–558.
67. Kamatari YO, et al. (2001) Response of native and denatured hen lysozyme to high pressure studied by $^{15}N/^{1}H$ NMR spectroscopy. *Eur J Biochem* 268(6):1782–1793.
68. Matthews BW (2012) Proteins under pressure. *Proc Natl Acad Sci USA* 109(18):6792–6793.
69. Refaee M, Tezuka T, Akasaka K, Williamson MP (2003) Pressure-dependent changes in the solution structure of hen egg-white lysozyme. *J Mol Biol* 327(4):857–865.
70. Dahlhoff E, Somero GN (1991) Pressure and temperature adaptation of cytosolic malate dehydrogenase of shallow and deep-living marine invertebrates: Evidence for high body temperatures in hydrothermal vent animals. *J Exp Biol* 159(1):473–487.
71. Rupley JA, Careri G (1991) Protein hydration and function. *Adv Protein Chem* 41:37–172.
72. Pikuta EV, et al. (2007) *Thermococcus thioreducens* sp. nov., a novel hyperthermophilic, obligately sulfur-reducing archaeon from a deep-sea hydrothermal vent. *Int J Syst Evol Microbiol* 57(Pt 7):1612–1618.
73. Chu XQ, Mamontov E, O'Neill H, Zhang Q (2012) Apparent decoupling of the dynamics of a protein from the dynamics of its aqueous solvent. *J Phys Chem Lett* 3(3):380–385.
74. Azuah RT, et al. (2009) DAVE: A comprehensive software suite for the reduction, visualization, and analysis of low energy neutron spectroscopic data. *J Res Natl Inst Stand Technol* 114(6):341–358.
75. Doster W, Cusack S, Petry W (1989) Dynamical transition of myoglobin revealed by inelastic neutron scattering. *Nature* 337(6209):754–756.